EGYPTIAN JOURNAL OF BOTANY (EJBO)

Print ISSN: 0375-9237
Online ISSN: 2357-0350

Spatial pattern and satellite radiometric indices of *Avicennia marina* populations in different habitat types of South Sinai, Egypt

Ahmad K. Hegazy, Mohamed Elhag, Hanan F. Kabiel, Merit Rostom, Samar S. Marae, Hossam E.A. Awad

PUBLISHED BY
THE EGYPTIAN
BOTANICAL SOCIETY

Spatial pattern and satellite radiometric indices of *Avicennia marina* populations in different habitat types of South Sinai, Egypt

Ahmad K. Hegazy[1], Mohamed Elhag[2,3], Hanan F. Kabiel[1], Merit Rostom[4], Samar S. Marae[1], Hossam E.A. Awad[1]

[1]*Botany and Microbiology Department, Faculty of Science, Cairo University, Giza, Egypt*

[2]*Department of Hydrology and Water Resources Management, Faculty of Meteorology, Environment and Arid Land Agriculture, King Abdulaziz University, Jeddah 21589, Saudi Arabia*

[3]*The State Key Laboratory, of Remote Sensing, Aerospace Information Research Institute, Chinese Academy of Science, Beijing 100101, China*

[4]*Academy of Scientific Research and Technology (ASRT), Egypt*

Urban mangroves, i.e., forests in and around cities are increasingly threatened, particularly for biodiversity conservation and sustainable use. A field study on the spatial pattern of *Avicennia marina* populations and satellite radiometric indices data analysis was carried out in different habitat types of Nabq protected area, Egypt. This study aims to assess *A. marina* populations and their spatial distribution pattern based on synchronized remote sensing image analysis and Ripley's k-function. The intertidal and shoreline habitats exhibited higher densities and healthier mangrove stands compared to the salt flats and sand mound habitats. The spatial pattern of *A. marina* tends to be aggregated for the populations established in almost all the study habitat types. Individuals in the sand mound and salt flat populations are more widely distributed than in the shoreline and intertidal populations. Two levels of aggregation are recognized: at fine scale (<1.5 m), and at coarse scale (>3.5 m). The seedlings and juveniles showed positive associations with the large-size individuals. The integration of remote sensing multiple indices and analyzing spatial and temporal patterns is an important tool for assessing and monitoring the overall health of mangrove forests for conservation and sustainable use.

Keywords: Population health, radiometric indices, Ripley's k-function, size classes, seedlings, pneumatophores

ARTICLE HISTORY
Submitted: June 15, 2024
Accepted: October 31, 2024

CORRESPONDENCE TO
Ahmad K. Hegazy,
Botany and Microbiology Department,
Faculty of Science, Cairo University,
Giza, Egypt
Email: hegazy@sci.cu.edu.eg

DOI: 10.21608/ejbo.2024.297761.2890

EDITED BY: F. Salama

INTRODUCTION

Mangrove forests are mainly found on the coasts and islands of the tropical and subtropical regions and provide goods and support invaluable biological, ecological, and economic services for people. Besides the coastal protection, mangrove ecosystems provide important coastal carbon sink amounted to five times higher than the total carbon storage per unit area basis in temperate, boreal, and tropical terrestrial forests (Daniel et al., 2011; Howard et al., 2017). As a conservation demand to ensure sustainable provision of goods and services, it is important to understand the variations of mangrove vegetation and populations across the landscape and habitat types to successfully manage the ecosystem resources (Wood et al., 2018).

Coastal wetlands in South Sinai are susceptible to sea-level rise and are considered a critical step in the leveling and filling of coastal depressions. In the Nabq protected area, the existence of mangrove habitat types depends on the balance between sea level and tidal sediment accumulation, which is governed by tidal exposure. The expected sea-level rise may result in mangrove retreat towards the shoreline and landward due to inundation. This scenario is reflected in population demography and spatial patterns.

Urban mangroves, i.e., forests in and around cities (*senso* Chow, 2018) are increasingly regarded as emerging environmental issues, particularly for biodiversity conservation and sustainable use (Branoff, 2017; Tuholske et al., 2017), supporting capture fisheries activities and traditional cultural functions such as recreation, inspiration, and education (Friess et al., 2019). In south Sinai, the natural mangrove ecosystem is found in the Nabq protected area and Ras Mohamed is close to Sharm El-Sheikh city and is threatened by the intensity of urbanization and the changing landscape due to the establishment of sea-side resorts and tourism activities. Accordingly, it is important to assess the soil, vegetation, and water radiometric indices and spatial patterns of *Avicennia marina* that support the conservation and development plans in the region to ensure the continued provision of mangrove goods and services in this multifunctional ecosystem.

Satellite remote sensing is low-cost, accurate, and rapid method to produce mangrove forest maps (Friess et al., 2019), remote sensors can directly measure land cover, land surface reflectance, land surface temperature, vegetation properties, and soil characteristics (Elhag, 2016). In literature, ongoing efforts are reported on the development of new algorithms that rely on satellite remote sensing data

and image processing techniques to estimate soil, water, and vegetation variables (Boegh et al., 2004; Panda et al., 2010). The remote sensing data as derived for natural vegetation resource management include biomass accumulation and plant growth (Ines et al., 2006), crop water parameters (Blaes and Defourny, 2003) and crop coefficients, and water productivity indicators (Karatas et al., 2009).

This study aims to assess the characteristics of mangrove populations and to identify the spatial distribution of *Avicennia marina* populations in different habitat types based on synchronized remote sensing image analysis and Ripley's k-function for studying the spatial pattern. The application of Remote Sensing and GIS technology for monitoring the mangrove populations and vegetation provides useful information for planning conservation and the rehabilitation of mangrove ecosystems.

MATERIAL AND METHODS

Study area

The study area is in Nabq protectorate, Gulf of Aqaba, south-east Sinai Peninsula, Egypt (Marae and Hegazy, et al. 2024). Mangrove stands situated on the seaward ends of Wadi Kid and Wadi Um A'dawy. Four main sites occur in the region, viz., Gharquana, Abu Zabad, Rowaisseya, and Monquatea which represent the most northern limit for mangrove distribution in the Red Sea and Indian Ocean. Four habitat types are found in the study area where mangrove vegetation is established: Shoreline, intertidal, sand mounds, and salt plain. The elevated patches in the salt plain and sand mounds support scattered *A. marina* plant growth.

The mountain ranges on the eastern and western sides of the Red Sea extending from south to north parallel to the coast have created a climatic tropical corridor that facilitates the migration of some tropical species to the subtropical region of south Sinai Peninsula (Hegazy and Amer, 2003). South Sinai region is positioned at the point of intersections of four biogeographical regions: Mediterranean, Irano-Turanean, Saharo-arabian, and Sudanian regions. This is reflected in its habitat and floristic diversity where many tropical species escaped and established in the region including *Avicennia marina*, *Moringa perigrina*, *Salvadora persica*, *Acacia tortilis*, *Suaeda monoica,* and *Hyphaene thebaica*.

Mangrove vegetation occurs as mono-specific stands of the grey mangrove, *Avicennia marina* (Forssk.) Vierh., growing on Pliocene fossil reefs (3.4-5.2 million years ago) and associated deposits, as well as on recent sub-fossil coral reefs (Evenari et al., 1985; Mashaly et al., 2012). Soil salinity in the study area may reach as high as 4.7% and the average air temperature is variable with values ranging between 15-19oC in winter and 20-32oC in winter. The annual average air temperature is 26 °C (Mashaly et al., 2012).

Field Work

Plant populations in different sites and habitat types were monitored for different functional traits. The adult plant density in every population was estimated as a number per square 100-meter, the density of seedlings as a number per square meter, the average tree height in meters, and the percentage of plant cover as estimated by the line intersect method, The number of respiratory roots (pneumatophores) as number per square meter, the root length in centimeters, and percentage of root deformations were estimated.

Spatial pattern analysis

Ripley's k-function was used to study the spatial pattern of *A. marina* populations (univariate analysis) and the spatial relationship between pairs of size classes (bivariate analysis) in the four study populations (Haase, 1995; Hegazy and Kabiel, 2007). The spatial pattern analysis was estimated by using a computer program (SPPA) following Haase (2002) and Hegazy *et al*. (2014).

K-function [k(d)] is a function of the mean number of neighbors over all individuals at the distance d; $k(d) = n^{-2}\, A \sum_{i=1}^{n} \sum_{j=1}^{n} wij \cdot I_d(i,j)$, i ≠ j, where n is the number of individuals in the area A, wij is a weighting factor used to reduce the problem of the edge effect. Id takes the value 1 if the distance between i and j is less than d, and the value 0 otherwise. The L-function; $L(d) = \sqrt{k(d)/\pi} - d$, is used by normalizing the K-function for simpler interpretation. In a univariate analysis, values of L(d) > 0 indicate a clumped pattern i.e., a greater number of individuals than would be expected if the individuals were randomly distributed. L(d) < 0 indicates a regular pattern i.e., fewer individuals within a scale than would be expected if the individuals were randomly distributed. In a bivariate analysis, L(d) > 0, the two size classes are aggregated and L(d) < 0 indicates that the two size classes are segregated within the scale d. Monte Carlo simulations were performed to estimate the

confidence intervals of the L-function for a 0.05 significance level.

Remote Sensing data

A synchronized image to the field data collection date (March 16th, 2021) was acquired from the European Space Agency hub to download a full-resolution Sentinel-2 image. Sentinel-2 image is composed of 13 spectral bands with spatial resolution ranges from 10 to 60m; most of these bands were used in the current study to estimate the different radiometric indices. The downloaded scene is corrected radiometrically and atmospherically from the source, so there was no need to perform any additional image correction techniques (Aljahdali and Elhag, 2020).

Soil Radiometric Indices

Brightness Index (BI), which is a sensitive algorithm to the soil's brightness based on soil surface salt accumulation. The BI can be estimated according to Escadafal, (1989) as follows:

$$BI = sqrt\left(\left(\left(red\_factor * red * red\_factor * red\right) + \left(green\_factor * green * green\_factor * green\right)\right) / 2\right)$$

Redness Index (RI), which is an algorithm developed by Pouget et al. (1990) to detect soil color variations. The RI can be estimated as follows:

$$RI = \left(red\_factor * red * red\_factor * red\right) / \left(green\_factor * green * green\_factor * green * green\_factor * green\right)$$

Vegetation Radiometric Indices

The red-Edge Inflection Point Index (REIPI), which is a Nitrogen uptake sensitive algorithm as an indication of vegetation health, it was introduced by Baret and Guyot, (1991). The REIPI was estimated as follows:

$$REIPI = 705 + 35 * (B4 + B7)/2 - B5) / (B6 - B5).$$

Weighted Difference Vegetation Index (WDVI) is an unrestricted range of the Perpendicular Vegetation Index that is very sensitive to atmospheric variations. WDVI can be estimated according to Clevers (1988) as follows:

$$WDVI = \left(IR\_factor * near\_IR - g * red\_factor * red\right)$$

Water Radiometric Indices

Normalized Difference Water Index (NDWI), which is a sensitive algorithm to detect water in vegetational canopies with less atmospheric interference. The NDWI was initially developed by Gao (1996), and can be estimated as follows:

$$NDWI = \left(IR\_factor * near\_IR - mir\_factor * middle\_IR\right) / \left(IR\_factor * near\_IR + mir\_factor * middle\_IR\right)$$

Modified Normalized Difference Water Index (MNDWI), which is an advanced version of the NDWI developed to suppress the effect of the surrounding vegetation and soils. The MNDWI was developed by Xu, (2006), and can be estimated as follows:

$$MNDWI = \left(green\_factor * green - mir\_factor * middle\_IR\right) / \left(green\_factor * green + mir\_factor * middle\_IR\right)$$

RESULTS

Spatial pattern

whole population pattern

In each of the four study populations, the whole pattern of *A. marina* tended to be aggregated at least at one distance scale, in alternation with random distribution (Figure 1). Clumped pattern was detected at 0.6-1.2m and 3.8m in the shoreline population (Figure 1a). In the intertidal population, the clumped pattern could be observed at 3.6m and most pronounced at greater than 4m (Figure 1b). The sand dune population showed significant aggregation at 1.1-1.4m (Figure 1c). The salt march population aggregation at 4.1-4.2m (Figure 1d). The minimum separation distance (MSD), where [(L(d)= -d, means no individuals occurred], between individuals increased from 0.2m and 0.1m in the shoreline and intertidal populations respectively (Figure 1a and b), to 0.4m in the sand dune and salt march populations. This indicates more widely distributed individuals in the latter populations.

Patterns within adult-size classes

In the shoreline population (Figure 2a-c), the medium-sized individuals were closer to each other (MSD = 0.4m) as compared to small and large-sized classes (MSD= 0.8 and 1.0m respectively). Individuals in the medium size class showed aggregation at 0.8-1.7m, compared to marginal aggregation at 1m in the small size class, and random distribution at all scales in the large size class.

For the intertidal population (Figure 2d-f), individuals in the small, medium, and large size classes were randomly distributed at all scales. Individuals in the small size class are closer to each other with an MSD of 0.1m compared to MSDs of 0.3 and 2.0m in individuals in medium and large size classes respectively.

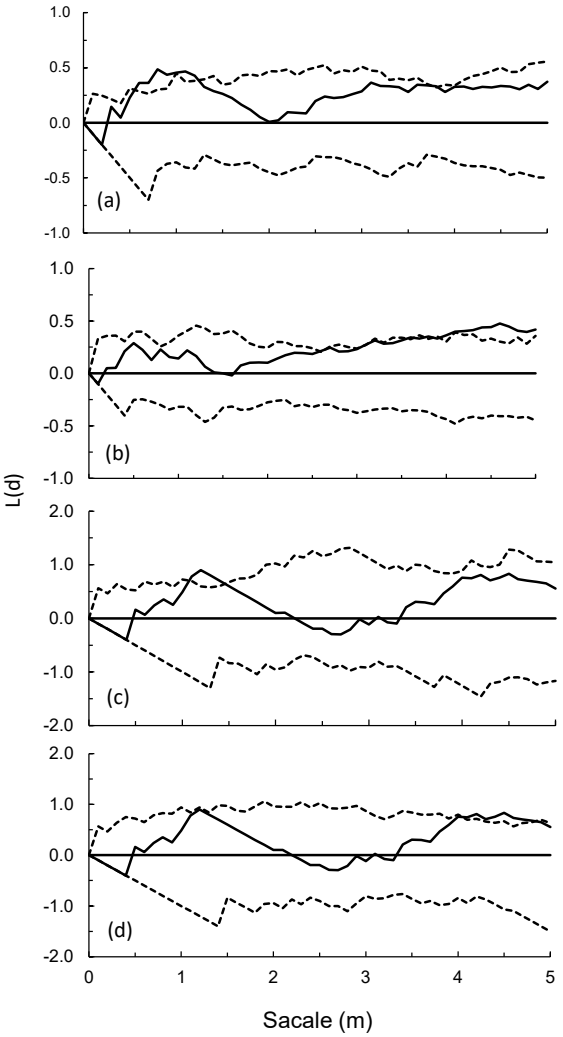

Figure 1. The statistics L(d) testing the spatial pattern of *Avicennia marina* at the individual level in shoreline (a), intertidal (b), sand dunes (c) and salt plain (d) zones.

Random distributions in all size classes were observed at all scales for the sand dune (Figure 2g-i) and salt march populations (Figure 2k-m), except for a marginal aggregation of medium-size class individuals at 3.2-3.8m (Figure 2h). The highest MSDs (3.8 and 4.4m) were observed in the sand dune and salt march populations (Figure 2i-m). In the sand dune population, the MSD decreased from 1.9m in the small size class to 0.9m in the medium size class (Figure 2g, h). While in the salt march population, the MSD increased from 0.4 m in the small size class to 0.6m in the medium size class (Figure 2k, l).

Pattern between adult-size classes

An overall random distribution was observed between pairs of size classes in the shoreline population (Figure 3a-c), except for a positive association between small and large individuals at 1.2m scale (Figure 3b). The small and medium individuals were closer to each other (MSD= 0.5m) than to large individuals with MSD of 1m between small and large individuals and 0.7m between medium and large individuals (Figure 3a, c).

As appears in the intertidal population (Figure 3d-f), small and medium individuals showed positive association at 0.8m and are closer to each other (MSD= 3m) compared to 1.0m between small and large individuals and 0.9m between medium and large individuals respectively. On the other hand, medium individuals showed a positive association with large individuals at 2.3 and 4.4m (Figure 3f).

The sand dune population showed a positive association between small and medium-size individuals at 1.1-1.2m and 4.1m with an MSD of 0.5m (Figure 3g). Small and large individuals, and medium and large individuals were more spaced with MSDs of 1.0 and 1.8m respectively (Figure 3h, i). The small individuals were closer to large individuals (positive association at 1.2m) than do medium individuals (Figure 3h).

In the salt march population, medium and large-size individuals were positively associated at 3.9-4m and showed the least MSD (0.7m) compared to 2.8m between small and large individuals and 0.7m between medium and large individuals (Figure 3k-m). An MSD of 2.8m between small and large individuals indicates a comparatively maximum separation distance between pairs of size classes or within size class in the study populations.

Pattern within seedlings and juveniles

Seedlings and juveniles were recorded only in the shoreline and intertidal populations. Seedlings were randomly distributed in both populations with small numbers: only 2 seedlings/10m^2 in the shoreline population and 3 seedlings/10m^2 in the intertidal population. For this, the MSD was found to be greater than the maximum scale used (5m) in the shore zone. In the intertidal population, the MSD within seedlings amounted to 3.1m (Figure 4a, b).

The juveniles were closer together in the shoreline population (MSD= 0.2m) compared to the intertidal population with an MSD of 1.0m (Figure 4c, d). They were clumped at 0.3-1.0m in the shoreline population and showed random distribution in the intertidal population. The spatial relationships between seedlings and juveniles were random with an MSD of 1.6 m in both populations (Figure 4e, f).

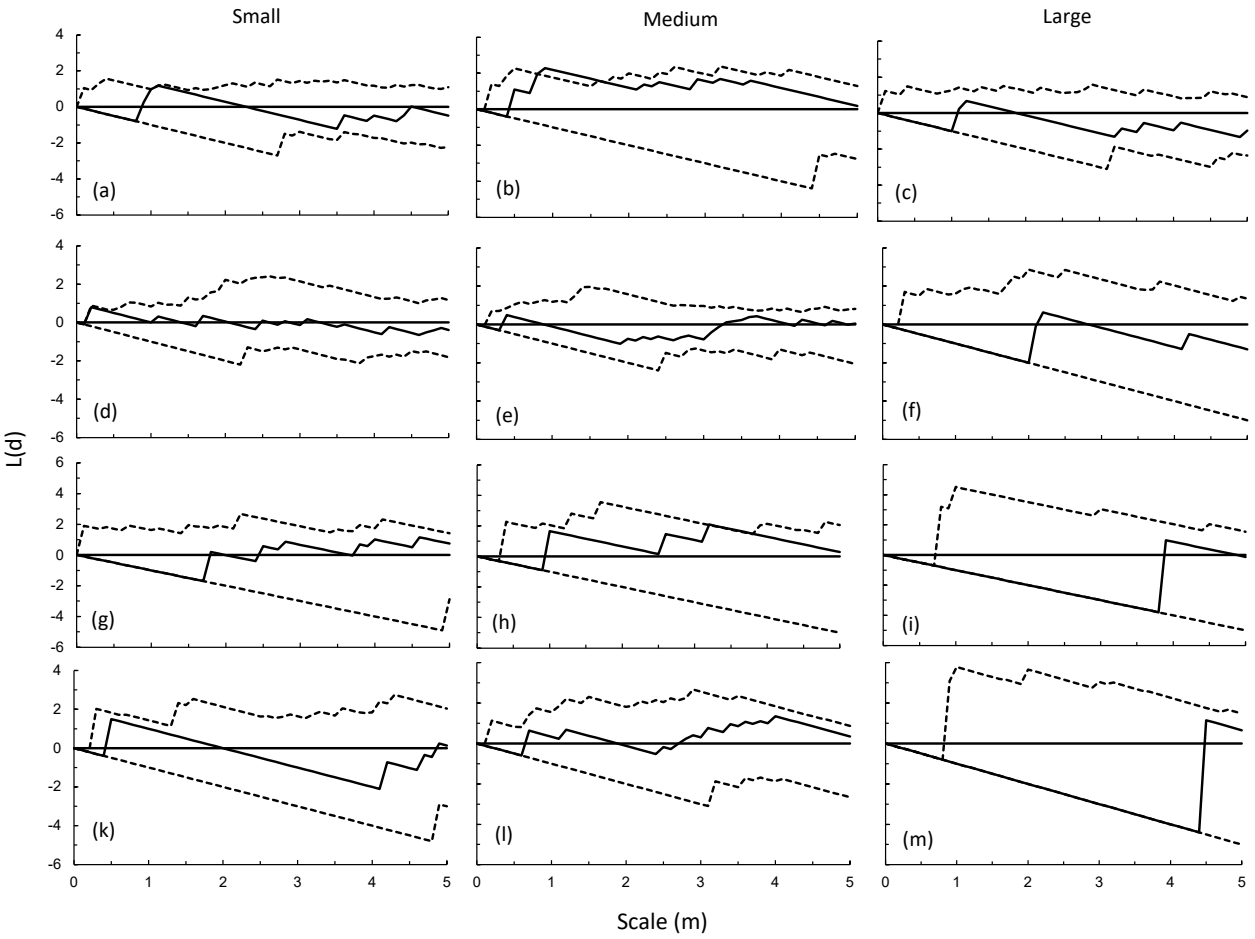

Figure 2. The spatial distribution of *Avicennia Marina* adult trees at the within size class level in shoreline (a, b, c), intertidal (d, e, f), sand dunes (g, h, i) and salt plain (k, l, m) zones.

Pattern between seedlings and juveniles and adult-size classes

Seedlings showed no association with small and medium size individuals in the shoreline and intertidal populations (Figure 5a-d). The MSD between seedlings and small size class increased from 0.7m in the shoreline populations to 1.4m in the intertidal populations (Figure 5a,b). Similarly, the MSD between seedlings and medium size class increased from 0.4m in the shoreline populations to 0.7m in the intertidal populations (Figure 5c, d). The seedlings showed positive associations with large individuals in both shoreline and intertidal populations at scales of 1.1-1.2m and 0.5m respectively (Figure 5e,f). The MSDs were comparatively smaller: 0.5 and 0.4m in the shoreline and intertidal populations, respectively. These findings indicate maximum association between seedlings and large individuals compared to the other size classes.

Juveniles showed positive associations with all size classes in all populations (Figure 5g-m), except for the relationship with small individuals in the shoreline population where random distribution was observed with an MSD of 1.4m (Figure 5g). Juvenile and small individuals in the intertidal population were positively associated at 1.6-1.9m and 2.3-2.7m (Figure 5h). Juveniles and medium individuals are aggregated at 3.4-3.9m and 4.1-4.2m in the shoreline populations and at 4.6m in the intertidal population with the closer association in the latter population with smaller MSD (0.2m) compared to 0.5m in the former population (Figure 5i, k). Juveniles and large individuals are aggregated at 0.6-1m in the shoreline populations and at 0.8-0.9m in the intertidal population with closer association in the latter population, with smaller MSD (0.3m) compared to 0.4m in the former population (Figure 5i,k).

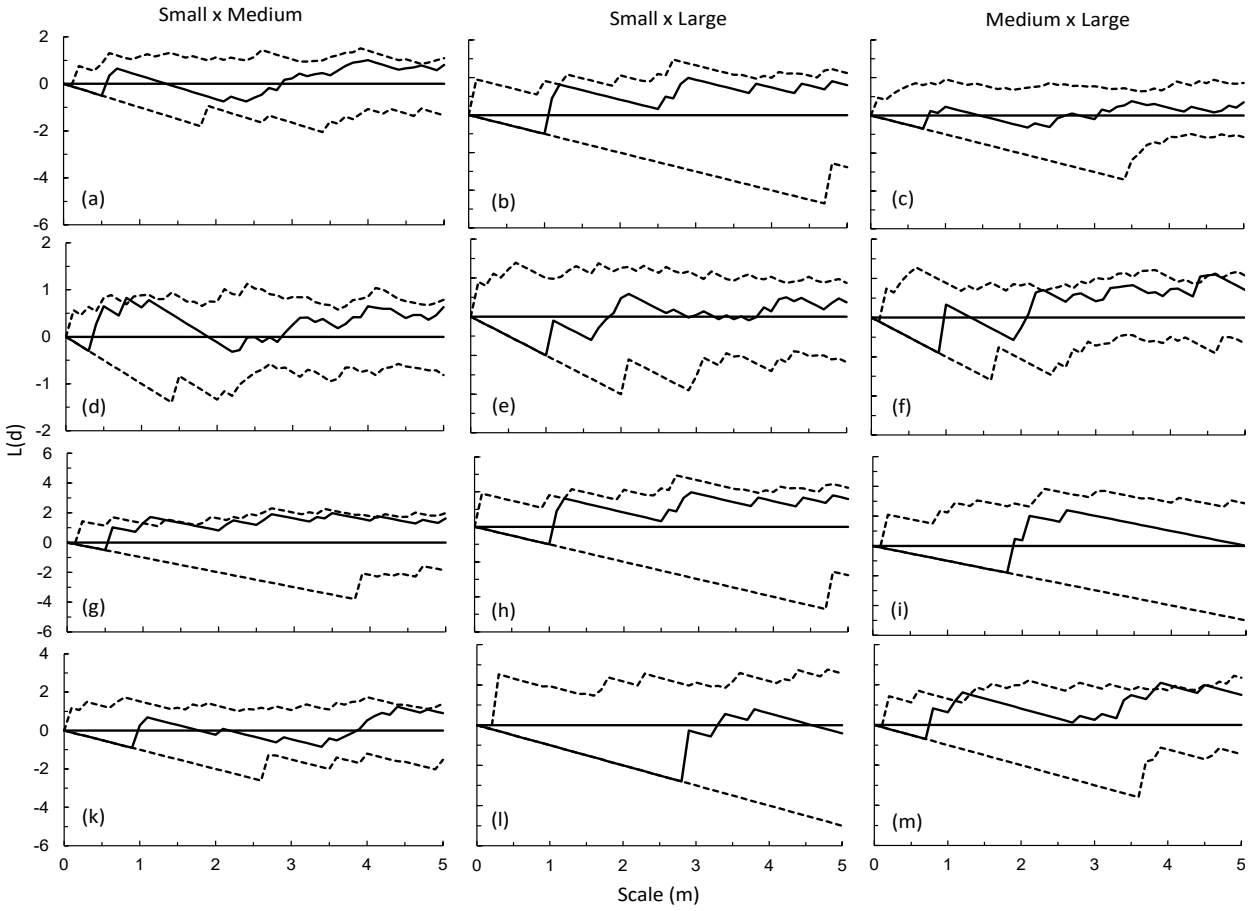

Figure 3. The spatial distribution of *Avicennia marina* adult trees at the between size class level in shoreline (a, b, c), intertidal (d, e, f), sand dunes (g, h, i) and salt plain (k, l, m) zones.

Remote sensing

Remote sensing data acquired from the Sentienl-2 sensor showed different regression analyses tested against the root deformation (%) and root length (cm). Three different radiometric indices (Soil, Vegetation, and Water Radiometric Indices) were derived from the remote sensing data to envisage the regression coefficient established between the remote sensing data and the tree health parameters of the examined mangrove stands. For each radiometric index, two different algorithms were used to realize the index. Brightness and Redness indices (Figure 6) as soil radiometric indices showed weak regressions (R^2= 0.69 and 0.58 respectively) with the mangrove deformation.

Vegetation radiometric indices showed better results than the soil indices (Figure 7). Specifically, the Weighted Difference Vegetation Index expressed in R^2 value of 0.814 which is the best inverted linear regression fit to represent the root deformation of mangrove. The response of the Red Edge Inflection Point Index and the mangrove root deformation was insignificantly correlated (R^2= 0.62).

Mangrove habitats are usually sited along the intertidal shorelines; therefore, the quest for Water Radiometric Indices realization is essential to envisage the association between the mangrove health parameters and the remotely sensed derivatives. The classic NDWI (Figure 8) failed to establish a consistent association with the tested mangrove root deformation (R^2= 0.48). On the other hand, the MNDWI proves its reliability to be used as an index to understand the linear regression between the Water Radiometric Index and the mangrove root deformation (R^2= 0.72).

The root length as a health parameter of the tested mangrove stands showed a stronger association with the different indices derived from the remote sensing data. Soil Redness Index (Figure 9) expressed a signification of a linear regression fit with R^2 value of

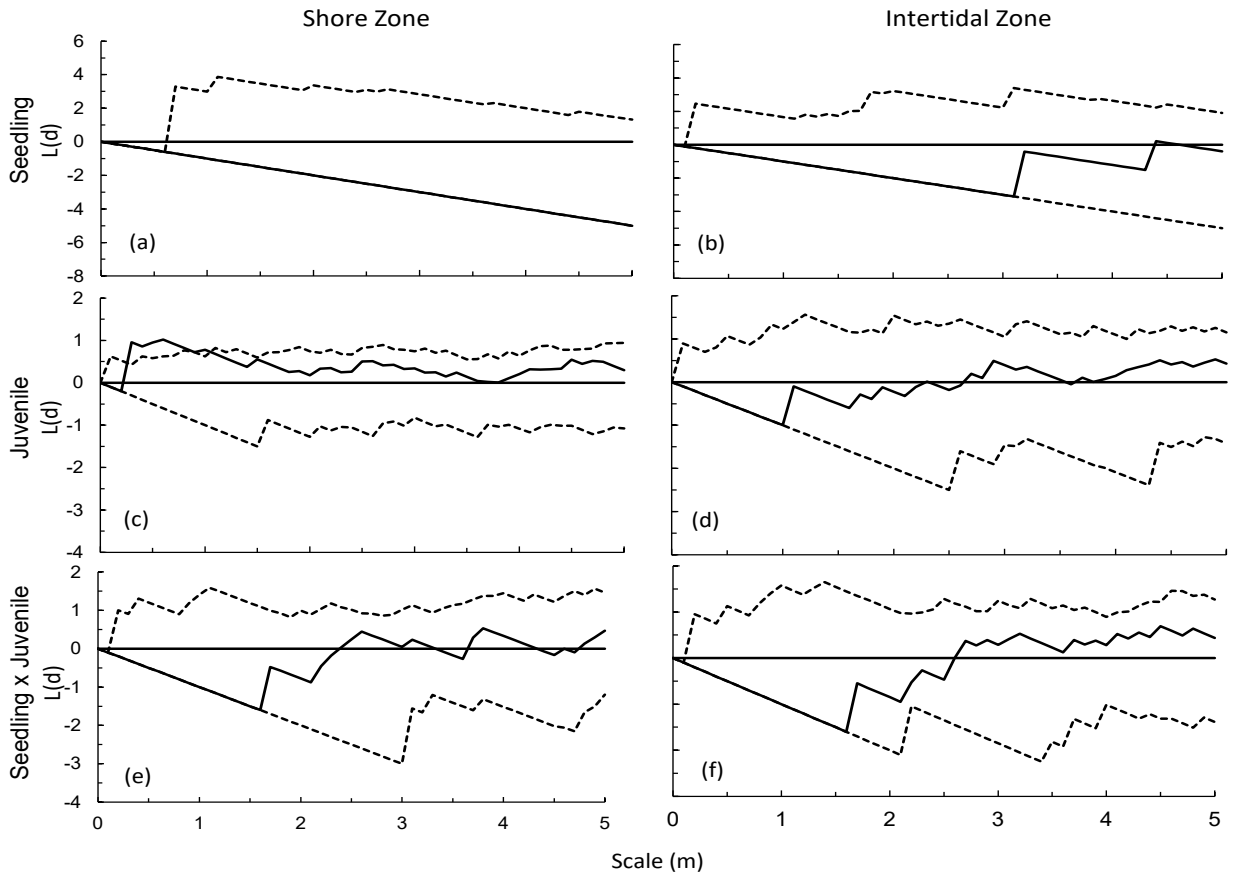

Figure 4. The spatial distribution of *Avicennia marina* seedling and juvenile individuals at the within and between size class level in shoreline and intertidal zones. The seedlings (a, b), juveniles (c, d), and seedlings and juveniles (e, f).

0.98, which is the best index to represent the mangrove health parameter and the scrutinized remote sensing derivative. The weighted difference vegetation index (MDVI) showed a significant correlation (Figure 10) with the root length (P value of 0.96).

Following the same pattern, Water Radiometric Indices (Figure 11) showed reliable associations with the mangrove root length rather than the root deformation. The classical NDWI expressed an insignificant difference between the R^2 value and the R^2 value of MNDWI, where the R^2 values of the NDWI and the MNDWI were counted as 0.94 and 0.93 respectively.

The person Correlation Coefficient with a P value of 0.95 significance was tested to study the correlation strength among the realized remote sensing indices and the mangrove health parameters. The root deformation correlation with the different radiometric indices showed a significant P value of 0.95 between the root deformation and the soil brightness index. The soil brightness index showed a significant correlation with the MNDWI.

The mangrove root length parameter showed different correlation behavior with the remote sensing data, where the WDVI was significantly correlated with the root length with P values of 0.96. The BI and the MNDWI are significantly correlated with a P value of 0.96.

The thematic mapping of the different radiometric indices implemented in this study (Figure 12) showed the location of the four mangrove stands, where the values of each radiometric group consider the soil, vegetation, and water radiometric indices.

Soil indices: The Brightness Index (BI) as shown in Figure 12a, is used to assess soil condition. The red brightness color is linked with soil humidity and the presence of salts in the soil, with a BI value of 0 indicating these conditions. The blue brightness indicates water bodies, with a maximum BI value. Figure 12b shows the Redness Index (RI), which also provides information about soil condition.

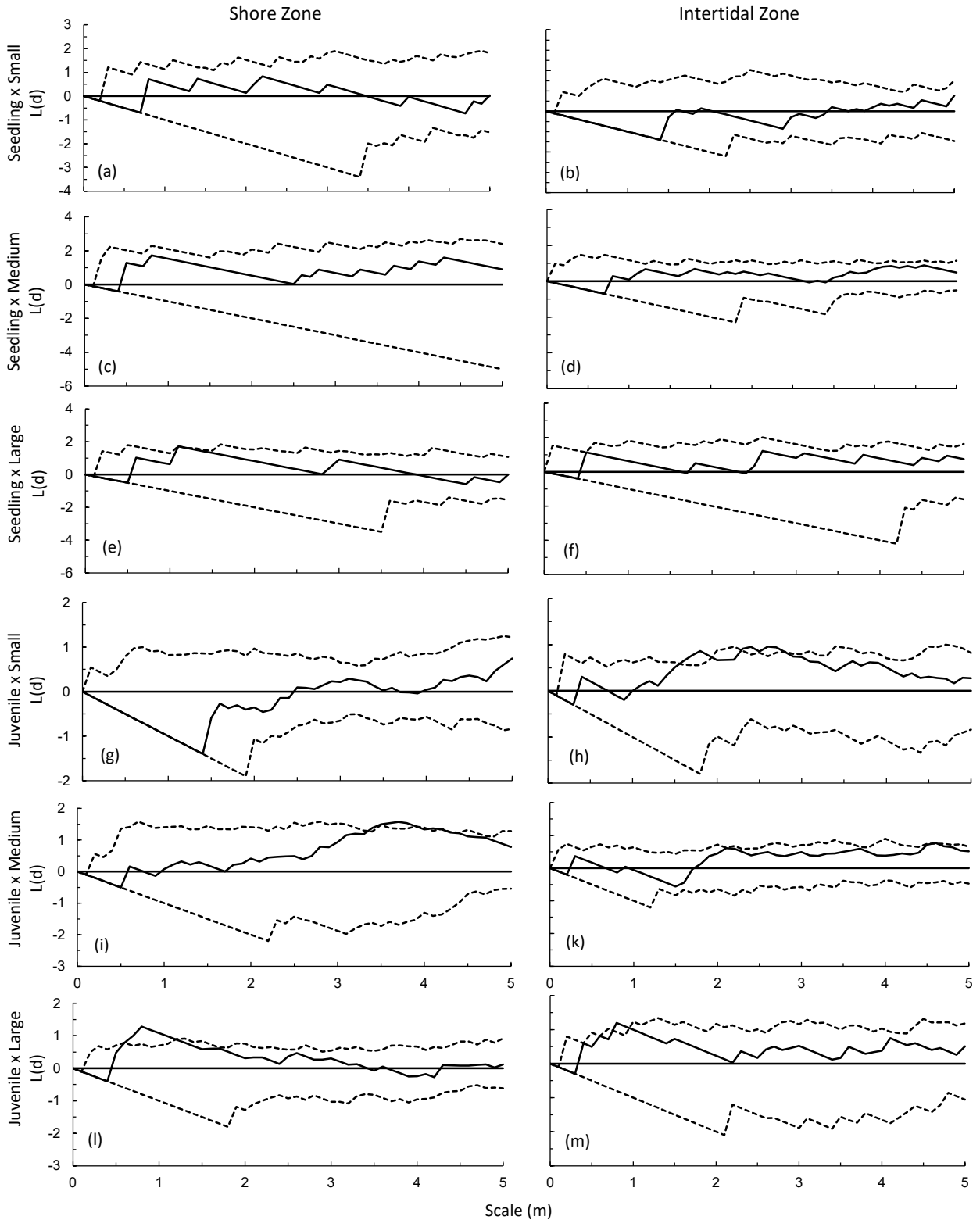

Figure 5. The spatial distribution of *Avicennia marina* seedlings and juvenile individuals at the between-size class level with large, medium, and small-size classes of adult individuals in shoreline and intertidal zones. The seedlings and small size class (a, b), seedlings and medium size class (c, d), seedling and large size class (e, f), juveniles and small size class (g, h), juveniles and medium size class (i, k), and juveniles and large size class (l, m).

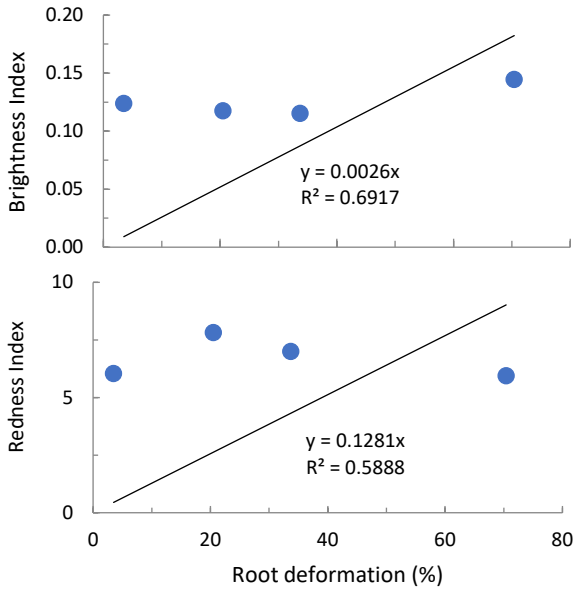

Figure 6. Regression analysis of soil brightness and redness radiometric indices against root deformation.

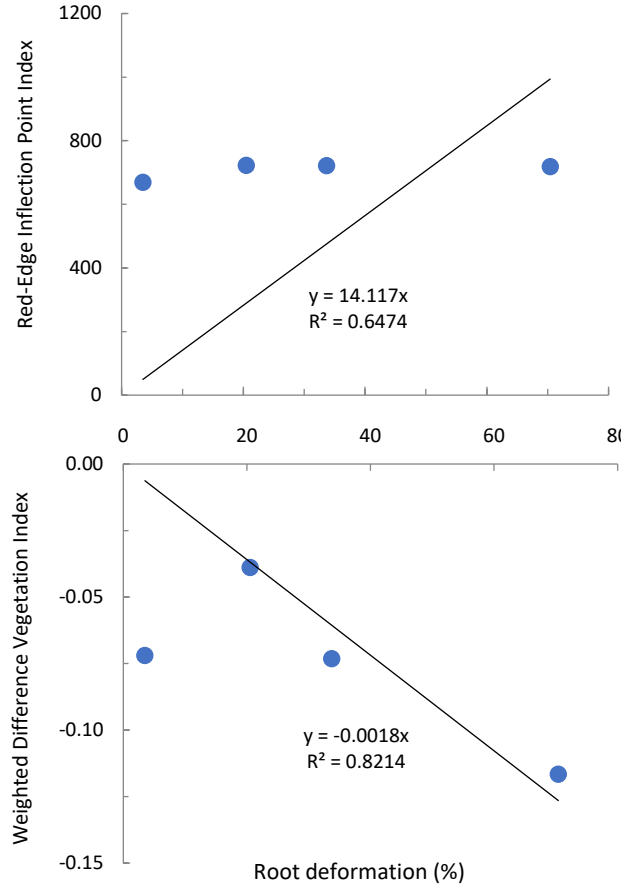

Figure 7. Regression analysis of vegetation red edge inflection point and weighed difference radiometric indices against root deformation.

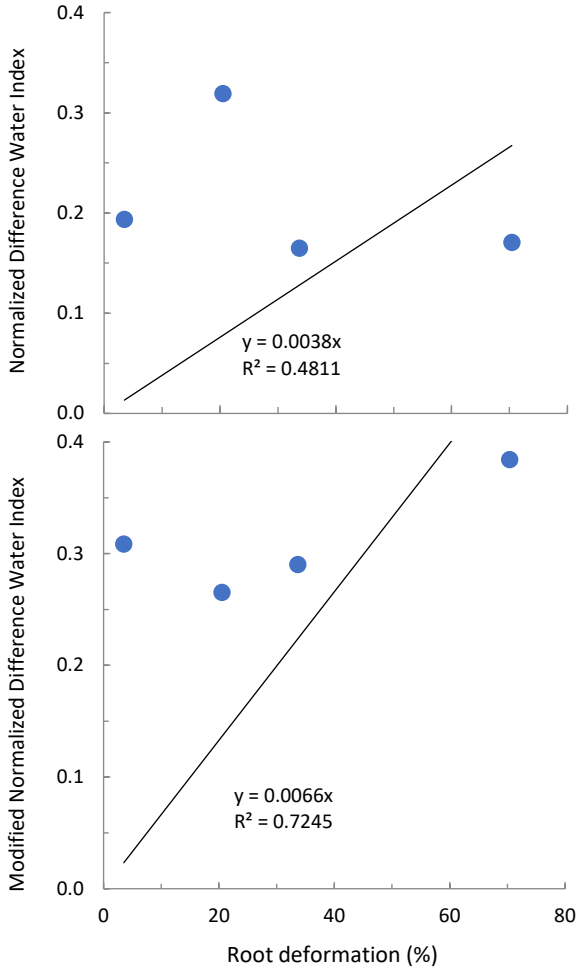

Figure 8. Regression analysis of normalized difference and modified normalized difference of water radiometric indices against root deformation.

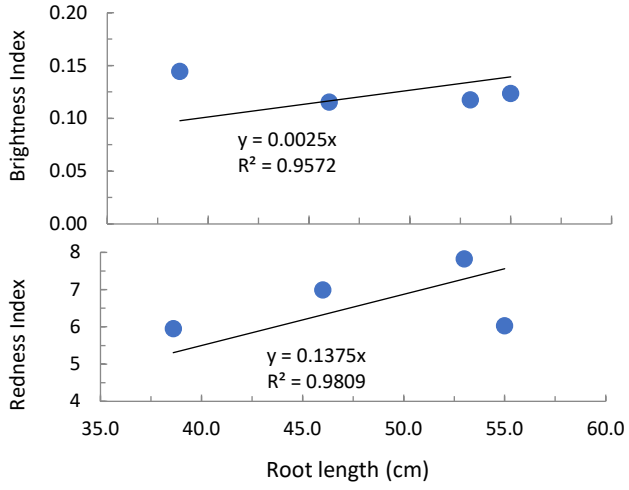

Figure 9. Regression analysis of soil brightness and redness radiometric indices against root length.

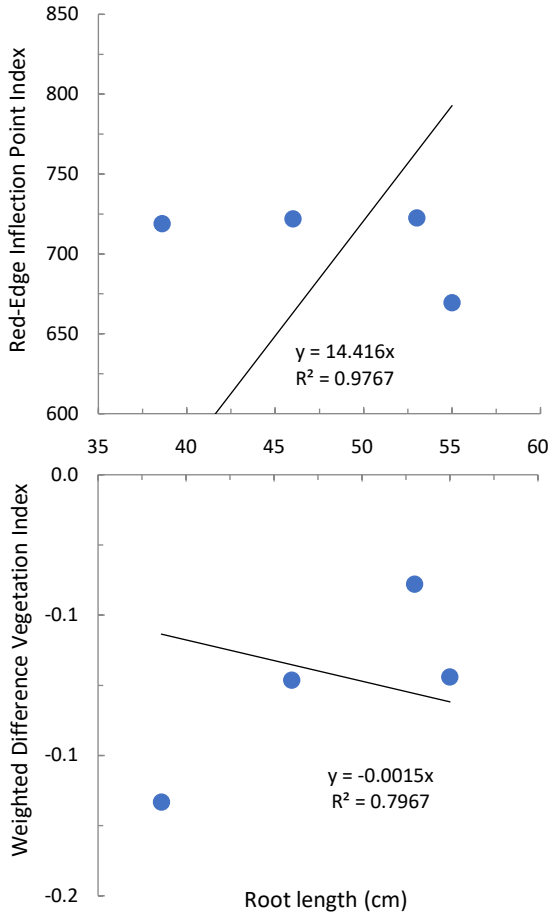

Figure 10. Regression analysis of vegetation red edge inflection point and weighed difference radiometric indices and root length.

The index ranges from 1 to -1, where 1 is the red brightness color that is linked with no soil color variation (i.e., a water body in the current study). The blue brightness towards -1 indicates the shallow shoreline.

Vegetation Indices: The Weighted Difference Vegetation Index (WDVI), which is used to assess vegetation conditions (Figure 12c), ranges from negative infinity (blue color) to positive infinity (red color), with the yellow tone indicating the algorithm's sensitivity to the current mangrove forests within the study area. Figure 12d shows the Red Edge Inflection Point Index (REIPI), which is another metric for evaluating vegetation conditions. The index ranges from -700 (blue color) to +700 (red color), where the blue color indicates nitrogen (N) uptake activities, and the red color suggests no nitrogen (N) uptake is possible.

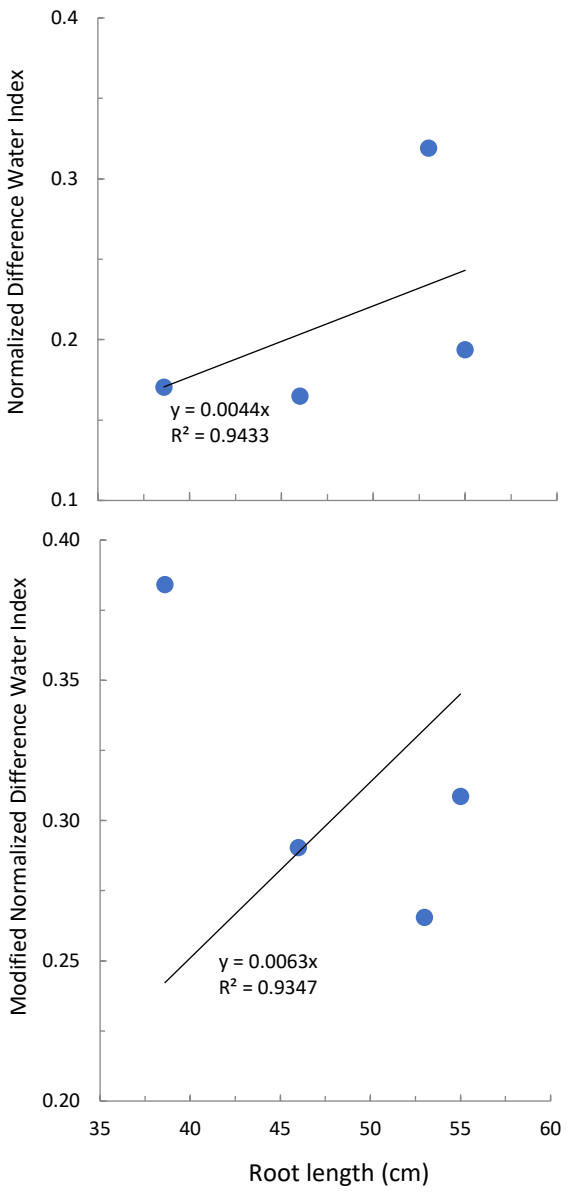

Figure 11. Regression analysis of normalized difference and modified difference water radiometric indices against root length.

Water Indices: The Normalized Difference Water Index (NDWI), which is used to assess canopy water content (Figure 12e), ranges from -1 (blue color for mostly dried vegetation) to +1 (red color that indicates the presence of water bodies). Figure 12f presents the Modified Normalized Difference Water Index (MNDWI), which is an enhancement of the NDWI. The MNDWI follows a similar color pattern to the NDWI, but it is designed to suppress built-up land noise as well as soil noise, leading to a more homogenous tone of red and blue brightnesses.

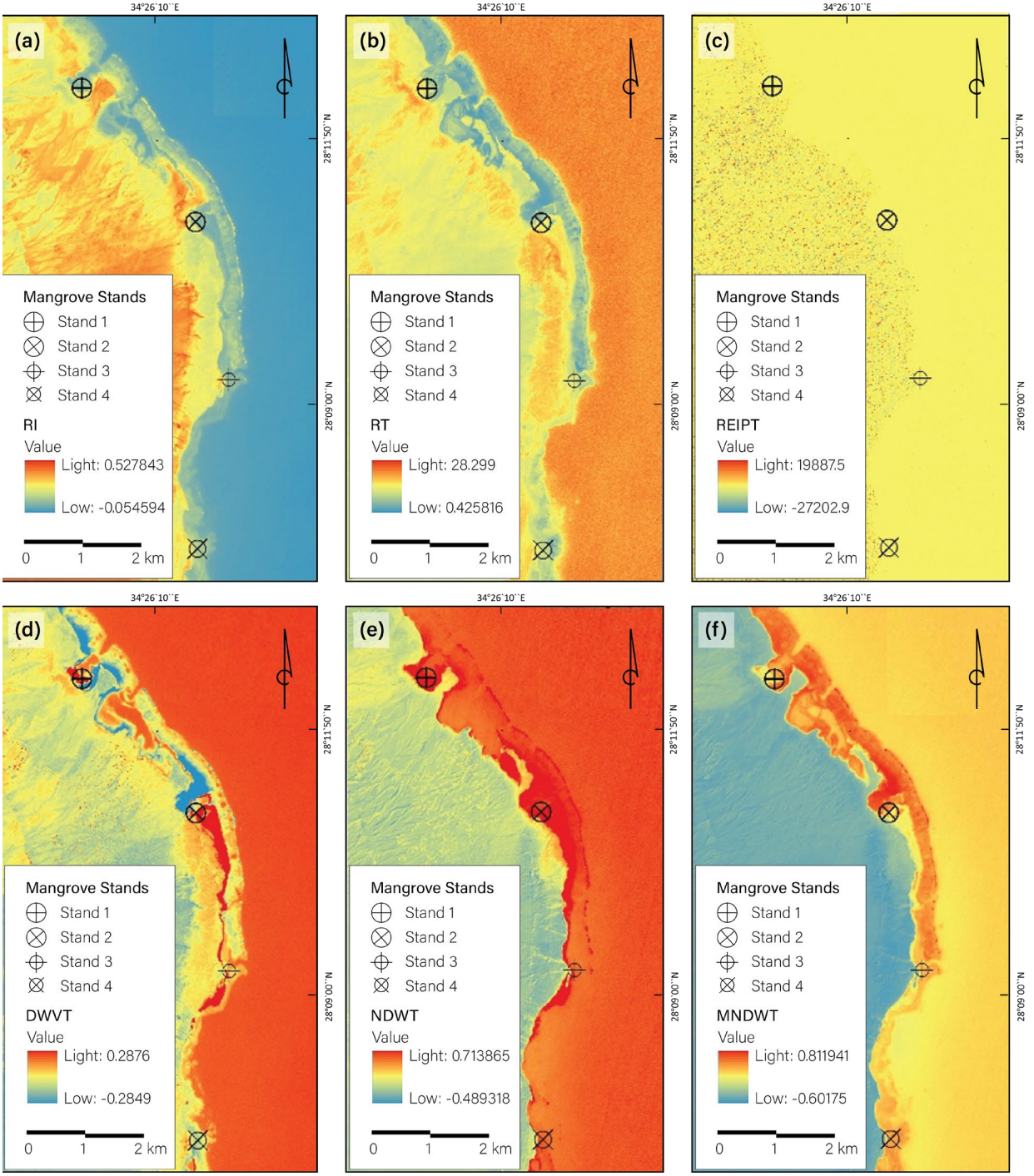

Figure 12. Maps of radiometric indices realization for mangrove health parameter assessment. a= soil brightness index (BI), b= soil redness index (RI), c= weighted difference vegetation index (WDVI), d= red edge inflexion points index (REIPI), e= normalized difference water index (NDWI), f= modified normalized difference water index (MNDWI)

DISCUSSION

Mangrove ecosystems supply multiple goods and services with trade-offs common between provisioning and regulating services (Castro et al., 2014; Raudsepp-Hearne et al., 2010). Managing multi-functionality, i.e., the capacity of an ecosystem to simultaneously produce multiple ecosystem services (Manning et al., 2018; Mastrangelo et al., 2014) may therefore be challenging if there are trade-offs in the supply of ecosystem services and the

spatial distribution of plant species (Villamagna et al., 2013). In the strict sense, trade-offs occur when the production of one service excludes or reduces the production of another service (Bennett et al., 2009). This is assessed by tree health and characteristics of the natural resources in the ecosystem (Alharthi et al. 2020). As commonly used in the wider ecosystem services literature, we use trade-off and synergy to refer to the directional relationship between pairs of co-occurring services, which may not be causally linked or may not respond to the same drivers. That is, tradeoffs occur when ecosystem services inversely co-vary with each other in space or time; and synergy occurs when ecosystem services co-vary in the same direction (Raudsepp-Hearne et al., 2010). In practice, these relationships are often conveyed as "ecosystem service bundles", which describe the overall pattern of interactions among multiple ecosystem services that spatially cluster in the landscape (e.g. Queiroz et al., 2015; Raudsepp-Hearne et al., 2010).

Spatial pattern

The spatial pattern of *A. marina* distribution tends to be aggregated for the populations established in the different habitat types of South Sinai, two levels of aggregation are recognized at; fine scale (<1.5 m), and at coarse scale (>3.5 m). This pattern reflected the facilitation offered by mother plants and could be rendered to the dispersal pattern of the species in the vicinity of the mother plant (Osunkoya and Creese1997, Baskin and Baskin 2001, Al-Qthanin, and Alharbi 2020, Alsamadany, et al. 2020). In the same context, seedlings and juveniles showed positive associations with the large-size individuals as compared to other medium- and small-size classes.

Individuals in the sand dune and salt march populations are more widely distributed than in the shoreline and intertidal populations. This could be rendered in part to the absence of seedlings and juveniles in the latter populations. The presence of suitable sites within a mosaic structure of abiotic resources, or restricted dispersal are probable reasons (Hegazy and Kabiel 2007, Schulze et al. 2019). Furthermore, the intensity of the clumped pattern (L(d) values) was greater in sand dunes and salt plain zones. The greater stress in the latter habitats, as compared to the shoreline and intertidal zones, could be a possible explanation for the facilitation (Qing et al., 2021).

The within-size class analysis indicated that medium-class individuals were comparatively closer to each other in the shoreline population, while individuals in the small-size class were closer to each other in the intertidal population. Alternatively, the among-size class analysis indicated that small and large individuals were closer to each other in the shoreline population, while small and medium individuals were closer to each other in the intertidal population. In both populations, the within-size class association was more powerful, indicating mass dispersal and germination, and successful recruitment in the vicinity of the mother plant in these habitats (Abo El-Nil 2001, Purnobasuki and Utami 2016). Seedlings and juveniles were found only in the shoreline and intertidal populations and represented by low numbers, 2-3 seedlings/10 m^2. The absence of seedlings and juveniles in the sand dune and salt plain populations reflected the stress of habitat conditions.

Remote sensing

Remote sensing radiometric indices are widely used in assessing the health and characteristics of various natural resources, including soil, vegetation, and water bodies. These indices provide valuable information about these resources' physical and biochemical properties, allowing researchers and environmental professionals to monitor and analyze their health and changes over time (Alharthi et al., 2020). When it comes to mangrove forests, remote sensing radiometric indices play a crucial role in assessing their health parameters (Elhag et al., 2021a).

Soil Indices: Remote sensing provides valuable insights into soil properties and characteristics using radiometric indices. One commonly used index is the Brightness Index (BI). BI considers the background soil reflectance and corrects it, making it suitable for areas with high soil brightness (Elhag et al., 2022). It helps in quantifying vegetation vigor and can be used to monitor soil degradation, erosion, and nutrient content in mangrove forests. Additionally, the Redness Index (RI) is another index that can be used to assess soil moisture content, which is vital for understanding the water availability and waterlogging issues in mangrove ecosystems. Soil Moisture and Nutrient Content can provide insights into soil moisture content and nutrient levels in mangrove forests. Changes in these indices can help identify soil degradation, erosion, or nutrient deficiencies (Elhag et al., 2020).

Vegetation Indices: Vegetation indices are widely used to assess the health, biomass, and productivity of vegetation, including mangrove forests. One of the most used vegetation indices is the Weighted

Difference Vegetation Index (WDVI). WDVI measures the difference between the reflectance in the near-infrared (NIR) and red spectral bands and provides an estimate of vegetation greenness and density. In mangrove forests, WDVI can be used to monitor changes in vegetation cover, identify stressed or damaged vegetation, and assess the overall health of the mangrove ecosystem (Hategekimana et al., 2020). Another important vegetation index is the Red Edge Inflection Point Index (REIPI), which improves the sensitivity to vegetation cover and reduces the atmospheric and background noise effects compared to NDVI. REIPI is particularly useful for mangrove forests with dense canopies, as it provides a more accurate measure of vegetation biomass and productivity (Shahbandeh and Elhag, 2023). Vegetation indices can be used to assess the density and coverage of mangrove vegetation. Decreased values of these indices may indicate stress, damage, or deforestation in the mangrove ecosystem. Vegetation indices can also provide estimates of biomass and productivity in mangrove forests. Changes in these indices over time can indicate variations in mangrove growth, primary productivity, or disturbances such as logging or pollution (Elhag et al., 2021b).

Water Indices: Remote sensing radiometric indices are also valuable in assessing water bodies, including mangrove wetlands. One of the commonly used water indices is the Normalized Difference Water Index (NDWI). NDWI measures the difference between the reflectance in the green and near-infrared spectral bands, allowing for the detection of water content. It can be used to monitor changes in water availability, identify waterlogged areas, and track the extent of flooding or drought stress in mangrove forests (Bahrawi et al., 2021). Furthermore, the Modified Normalized Difference Water Index (MNDWI) is another index specifically designed to highlight open water bodies while suppressing the influence of vegetation (Hussain et al., 2022a). MNDWI is useful in mangrove forests where water bodies are interspersed with dense vegetation cover. Water indices can help in monitoring water availability and identifying waterlogged areas within mangrove ecosystems. Reductions in water availability can indicate drought stress or alterations in hydrological regimes (Hussain et al., 2022b). By integrating multiple indices and analyzing their spatial and temporal patterns, it is possible to assess the overall health of mangrove forests.

Sudden changes or anomalies in these indices can indicate disturbances such as pollution, deforestation, or natural disasters (Kharazmi et al., 2023). The integration of remote sensing data with field surveys provided a comprehensive understanding of the mangrove ecosystem and its dynamics. The study highlighted the potential of remote sensing techniques for monitoring and assessing mangrove habitats on a larger scale, contributing to the development of effective conservation and sustainable use strategies.

The findings of the study revealed valuable insights into the spatial patterns of *A. marina* populations in the different habitat types. The intertidal and shoreline areas exhibited higher densities and healthier mangrove stands compared to the salt flats and sand mound habitats. Some factors, such as salinity, soil moisture, and tidal inundation played a role in shaping the local distribution patterns of *A. marina* populations. Further studies on integrating remote sensing and spatial pattern data are required to support the conservation and sustainable use of mangrove ecosystems in arid and semiarid subtropical regions.

ACKNOWLEDGMENT

We thank the rangers of the Nabq protected area for their help and guidance during the fieldwork.

COMPETING INTERESTS

Not applicable

AUTHORS' CONTRIBUTIONS

Conceptualization AKH. ME, SSM; Methodology and fieldwork, AKH, HEAA, SSM, MR; Data analysis: all authors. Manuscript drafting: AKH. ME, HFK, MR, HEAA; Review and editing: AKH, ME, MR. Overall guidance: AKH. All authors have read and agreed to the published version of the manuscript.

ETHICS APPROVAL

Not applicable

ABBREVIATIONS

BI: Soil Brightness Index
MNDWI: Modified Normalized Difference Water Index
MSD: Minimum Separation Distance
NDWI: Normal Difference Water Index
NIR: Near Infra-Red
REIPI: Red Edge Inflection Point Index
RI: Soil Redness Index
WDVI: Weighed Difference Vegetation Index

REFERENCES

AboEl-Nil, M.M. (2001) Growth and establishment of mangrove (*Avicennia marina*) on the coastlines of Kuwait. *Wetlands Ecology and Management*, 9, 421–428.

Alharthi, A., El-Sheikh, M.A., Elhag, M., Alatar, A.A., Abbadi, G.A., Abdel-Salam, E.M., Arif, I.A., Baeshen, A.A. and Eid, E.M. (2020) Remote sensing of 10 years changes in the vegetation cover of the northwestern coastal land of Red Sea, Saudi Arabia. Saudi Journal of Biological Sciences, 27, 3169-3179.

Aljahdali, M.H., Elhag, M. (2020) Calibration of the depth invariant algorithm to monitor the tidal action of Rabigh City at the Red Sea Coast, Saudi Arabia. *Open Geosciences*, 12, 1666-1678.

Al-Qthanin, R.N. and Alharbi, S.A. (2020) Spatial Structure and Genetic Variation of a Mangrove Species (*Avicennia marina* (Forssk.) Vierh) in the Farasan Archipelago. Forests (MDPI), 11, 1287; doi:10.3390/f11121287

Alsamadany, H., Al-Zahrani, H.S., Selim, E.M., El-Sherbiny, M.E. (2020) Spatial distribution and potential ecological risk assessment of some trace elements in sediments and grey mangrove (*Avicennia marina*) along the Arabian Gulf coast, Saudi Arabia. *Open Chemistry*, 18, 77–96.

Bahrawi, J., Alqarawy, A., Chabaani, A., Elfeki, A. and Elhag, M. (2021) Spatiotemporal analysis of the annual rainfall in the Kingdom of Saudi Arabia: predictions to 2030 with different confidence levels. *Theoretical and Applied Climatology*, 146, 1479-1499.

Baret, F., Guyot, G. (1991) Potentials and limits of vegetation indices for LAI and APAR assessment. *Remote Sensing of Environment*, 35(2),161–173.

Baskin CC, Baskin JM (2001) Seeds: ecology, biogeography, and evolution of dormancy and germination. Academic Press, San Diego.

Bennett, E.M., Peterson, G.D., and Gordon, L.J. (2009) Understanding relationships among multiple ecosystem services. *Ecology letters*, 12(12), 1394–1404.

Blaes, X., Defourny, P. (2003) Retrieving crop parameters based on tandem ERS 1/2 interferometryc coherence images. *Remote Sensing of Environment*, 88, 374–385.

Boegh, E., Thorsen, M., Butts, M.B., Hansen, S., Christiansen, J.S., Abrahamsen, P., Hasager, C.B., Jensen, N.O., van der Keur, P., Refsgaard, J.C., Schelde, K., Soegaard, H., Thomsen, A. (2004) Incorporating remote sensing data in physically based distributed agro-hydrological modelling. *Journal of Hydrology*, 287, 279-299.

Branoff, B.L. (2017) Quantifying the influence of urban land use on mangrove biology and ecology: a meta-analysis. *Global Ecology and Biogeography*, 26, 1339–1356.

Castro, A.J., Verburg, P.H., Martín-López, B., García-Llorente, M., Cabello, J., Vaughn, C.C. and López, E. (2014) Ecosystem service trade-offs from supply to social demand: A landscape-scale spatial analysis. *Landscape and Urban Planning*, 132, 102-110.

Chow, J. (2018) Mangrove management for climate change adaptation and sustainable development in coastal zones. *Journal of Sustainable Forestry*, 37, 139–156.

Clevers, J.G.P.W. (1988) The derivation of a simplified reflectance model for the estimation of leaf area index. *Remote Sensing of Environment*, 35, 53- 70.

Daniel, C.D., Kauffman, J.B., Murdiyarso, D., Kurnianto, S., Sthidham, M., and Kanninen, M. (2011) Mangroves among the most carbon-rich forests in the tropics. Nature Geosciences Letters, NGEO1123 (5pp).

Elhag, M. (2016) Evaluation of different soil salinity mapping using remote sensing techniques in arid ecosystems, Saudi Arabia. *Journal of Sensors*, 2016, ID 7596175, 8 pages.

Elhag, M., Boteva, S. and Al-Amri, N. (2021a) Forest cover assessment using remote-sensing techniques in Crete Island, Greece. *Open Geosciences*, 13, 345-358.

Elhag, M., Gitas, I., Othman, A., Bahrawi, J., Psilovikos, A. and Al-Amri, N. (2021b) Time series analysis of remotely sensed water quality parameters in arid environments, Saudi Arabia. Environment. *Development and Sustainability*, 23, 1392-1410.

Elhag, M., Hidayatulloh, A., Bahrawi, J., Chaabani, A. and Budiman, J. (2022) Using inconsistencies of wadi morphometric parameters to understand patterns of soil erosion. *Arabian Journal of Geosciences*, 15, 1299.

Elhag, M., Yimaz, N., Bahrawi, J. and Boteva, S. (2020) Evaluation of Optical Remote Sensing Data in Burned Areas Mapping of Thasos Island, Greece. *Earth Systems and Environment*, 4, 813-826.

Escadafal R. (1989) Remote sensing of arid soil surface color with Landsat thematic mapper. *Advances in Space Research*, 9,159-163.

Friess, D.A., Rogers, K., Lovelock, C.E., Krauss, K.W., Hamilton, S.E., Lee, S.Y., Lucas, R., Primavera, J., Rajkaran, A., Shi, S. (2019) The state of the world's mangrove forests: past, present, and future. *Annual Review of Environmental Resources*, 44, 89–115.

Evenari, M., I. Noy-Meir, I. and D.W. Goodall (eds) (1985) Ecosystems of the World, Volume 12A: hot deserts and arid shrublands. Amsterdam: Elsevier.

Gao, B. C. (1996) NDWI—a normalized difference water index for remote sensing of vegetation liquid water from space. *Remote Sensing Environment*, 58(3), 257–266.

Haase, P. (2002) Spatial Point Pattern Analysis (SPPA), computer program version 2.0, release December 2002.

Hategekimana, Y., Allam, M., Meng, Q., Nie, Y. and Elhag, M., (2020) Quantification of soil losses along the coastal protected areas in Kenya. *Land* (MDPI), 9(5), 137.

Hegazy, A.K., Kabiel, H.F. (2007) Significance of microhabitat heterogeneity in the spatial pattern and size-class structure of *Anastatica hierochuntica* L. *Acta Oecologica*, 31, 332-342.

Hegazy, A.K., Kabiel, H.F., Al-Rowaily, S.L., Faisal, M., Zayed, K., Doma, E. (2014) Temporal genetic and spatial pattern variations within and among *Anastatica hierochuntica* populations. *Rendiconti Lincei*, 25, 155–166

Hegazy, A.K. and Amer, W.M. (2003) Altitudinal and latitudinal diversity of the flora on the eastern and western sides of the Red Sea. Pp. 197-216. In B. Sener (ed.), *Biodiversity: Biomolecular Aspects of Biodiversity and Innovative Utilization*. London: Kluwer Academic/plenum Publishers. 426 pp.

Howard, J., Sutton-Grier, A., Herr, D., Kleypas, J., Landis, E., Mcleod, E., Pidgeon, E., Simpson, S. (2017) Clarifying the role of coastal and marine systems in climate mitigation. *Frontiers in Ecology and the Environment*, 15, 42–50.

Hussain, S., Bahrawi, J., Awais, M. and Elhag, M. (2022a) Understanding the role of the radiometric indices in temporal evapotranspiration estimation in arid environments. *Desalination Water Treatment*, 256, 221-234.

Hussain, S., Elfeki, A.M., Chaabani, A., Yibrie, E.A. and Elhag, M. (2022b) Spatio-temporal evaluation of remote sensing rainfall data of TRMM satellite over the Kingdom of Saudi Arabia. *Theoretical and Applied Climatology*, 150, 363-377.

Ines, A.V.M., Honda, K., Das Gupta, A., Droogers, P., Clemente, R.S. (006) Combining remote sensing-simulation modelling and genetic algorithm optimization to explore water management options in irrigated agriculture. *Agricultural Water Management*, 83, 221-232.

Karatas, B.S., Akkuzu, E., Unal, H.B., Asik, S., Avci, M. (2009) Using satellite remote sensing to assess irrigation performance in Water User Associations in the Lower Gediz Basin, Turkey. *Agricultural Water Management*, 96, 982–990.

Kharazmi, R., Rahdari, M.R., Rodríguez-Seijo, A. and Elhag, M. (2023) Long-term time series analysis of land cover changes in an arid environment using Landsat data: a case study of hamoun biosphere reserve, Iran. *Desert*, 28, 123-144.

Manning, P., van der Plas, F., Soliveres, S., Allan, E., Maestre, F.T., Mace, G., Whittingham, M.J. and Fischer, M. (2018) Redefining ecosystem multi-functionality. *Nature Ecology and Evolution*, 2(3), 427- 436.

Marae, S.S., Hegazy, A.K., Rostom, M., Hussein, Z.S., Awad, H.E.A (2024) Molecular Variations and Photosynthetic Pigment Content of *Avicennia marina* Growing in Subtropical Habitat Types. *Egyptian Journal of Botany,* 64, Special Issue, 16-28.

Mashaly, I.A., A.K. Hegazy and S.A. El-Hussieny (2012). Study of Mangrove (Avicennia marina (Forssk.) Vierh.) population demography in Nabq Protected Area, South Sinai. *Journal of Environmental Sciences*, Mansoura University, 41,401–425.

Mastrangelo, M.E., Weyland, F., Villarino, S.H., Barral, M.P., Nahuelhual, L. and Laterra, P. (2014) Concepts and methods for landscape multifunctionality and a unifying framework based on ecosystem services. Landscape Ecology, 29, 345–358.

Osunkoya, O.O. and Creese, R.G. (1997) Population Structure, Spatial Pattern and Seedling Establishment of the Grey Mangrove, *Avicennia marina* var. *australasica*, in New Zealand. *Australian Journal of Botany*, 45, 707–725.

Panda, S.S., Ames, D.P., Panigrahi, S. (2010). Application of Vegetation Indices for Agricultural Crop Yield Prediction Using Neural Network Techniques. *Remote Sensing*, 2, 673-696.

Pouget, M., Madeira, J., Le Floch, E. and Kamal, S. (1990) Título: Spectral characteristics of sandy surfaces in the north-western coastal region of Egypt: application to SPOT satellite data. In: *Journee de teledetection*, 12., 1990, Bondy, France. Characterizations and monitoring of terrestrial environments in arid and tropical regions. Paris, France: ORSTOM, 1991, pp 27–39.

Purnobasuki H. and Utami, E.S.W. (2016) Seed germination of *Avicennia marina* (Forsk.) Vierh. by pericarp removal treatment. *Biotropica*, 23, 74 – 83.

Qing, H., Zhao, L.-Q., Zhang, L., Yang, J., Huang, J.-H. (2021) Spatial pattern and association of shrub species in gravel hilly and rocky low mountain desert dominated by relict *Helianthemum songaricum* in China. *Global Ecology and Conservation*, 32, e01914.

Queiroz, C., Meacham, M., Richter, K., Norstrom, A.V., Andersson, E., Norberg, J. and Peterson, G. (2015). Mapping bundles of ecosystem services reveals distinct types of multifunctionality within a Swedish landscape. *AMBIO*, 44 (Suppl 1), 89–101.

Raudsepp-Hearne, C., Peterson, G.D., & Bennett, E.M. (2010) Ecosystem service bundles for analyzing tradeoffs in diverse landscapes. *Proceedings of the National Academy of Sciences of the United States of America*, 107(11), 5242–5247.

Schulze E.-D., Beck E., Buchmann N., Clemens S., Müller-Hohenstein K., Scherer-Lorenzen M. (2019) Plant Ecology. Second edition. chapter 18: Spatial Distribution of Plants and Plant Communities, pp.657-688. *Springer Nature*, Germany.

Shahbandeh, M. and Elhag, M. (2023) Microclimate changes and trend analysis of remotely sensed environmental parameters in West Asia Semi-arid region. *Environment, Development and Sustainability*, 25, 00-00.

Tuholske, C., Tane, Z., Lopez-Carr, ´ D., Roberts, D. and Cassels, S. (2017) Thirty years of land use/cover change in the Caribbean: Assessing the relationship between urbanization and mangrove loss in Roatan, Honduras. *Applied Geography*, 88, 84–93.

Villamagna, A.M., Angermeier, P.L. and Bennett, E.M. (2013) Capacity, pressure, demand, and flow: a conceptual framework for analyzing ecosystem service provision and delivery. *Ecological Complexity*, 15, 114–121.

Wood, S.L., Jones, S.K., Johnson, J.A., Brauman, K.A., Chaplin-Kramer, R., Fremier, A., Girvetz, E., Gordon, L.J., Kappel, C.V. and Mandle, L. (2018) Distilling the role of ecosystem services in the Sustainable Development Goals. *Ecosystem Services*, 29, 70–82.

Xu, H. (2006) Modification of normalized difference water index (NDWI) to enhance open water features in remotely sensed imagery. *International Journal of Remote Sensing*, 27(14), 3025-3033.